Available online at www.sciencedirect.com
SCIENCE DIRECT®
ELSEVIER
Nuclear Instruments and Methods in Physics Research A 525 (2004) 268–274
NUCLEAR INSTRUMENTS & METHODS IN PHYSICS RESEARCH Section A
www.elsevier.com/locate/nima

Novel design of a parallax free Compton enhanced PET scanner

A. Braem[a], M. Chamizo[b], E. Chesi[a], N. Colonna[c], F. Cusanno[d], R. De Leo[c], F. Garibaldi[d,*], C. Joram[a], S. Marrone[c], S. Mathot[a], E. Nappi[c], F. Schoenahl[e], J. Seguinot[a], P. Weilhammer[a], H. Zaidi[e]

[a] *CERN EP-Physics Division, CH-1211 Geneva, Switzerland*
[b] *University of Geneva, CH-1211 Geneva 4, Switzerland*
[c] *INFN, Sezione di Bari, Via Orabona 4, Bari, Italy*
[d] *Laboratory of Physics, ISS, Viale Regina Elena 299, Rome, Italy*
[e] *Division of Nuclear Medicine, Geneva University Hospital, CH-1211 Geneva, Switzerland*

Abstract

Molecular imaging by PET is a powerful tool in modern clinical practice for cancer diagnosis. Nevertheless, improvements are needed with respect to the spatial resolution and sensitivity of the technique for its application to specific human organs (breast, prostate, brain, etc.), and to small animals. Presently, commercial PET scanners do not detect the depth of interaction of photons in scintillators, which results in a not negligible parallax error. We describe here a novel concept of PET scanner design that provides full three-dimensional (3D) gamma reconstruction with high spatial resolution over the total detector volume, free of parallax errors. It uses matrices of long scintillators read at both ends by hybrid photon detectors. This so-called 3D axial concept also enhances the gamma detection efficiency since it allows one to reconstruct a significant fraction of Compton scattered events. In this note, we describe the concept, a possible design and the expected performance of this new PET device. We also report about first characterization measurements of 10 cm long YAP:Ce scintillation crystals.

Keywords: Positron emission tomography; Hybrid photodiode; Depth of interaction

1. Introduction

PET is a molecular imaging technique that uses radiolabelled molecules to image molecular biological processes in vivo [1,2]. A typical PET scanner consists of a planar ring of small photon detectors displaced radially (see Fig. 1), each in time coincidence with the others [1,2]. Two 511 keV photons simultaneously detected indicates the annihilation of a positron somewhere on the chord connecting the two involved detectors. The ensemble of the chords is the base of computed tomography (CT) in a single plane. Multiple detector rings, stacked each on top of the other, are used to obtain multiple sliced three-dimensional (3D) images.

*Corresponding author. Inst. Superiore de Sanita, INFN Roma1 gr. Sanita, Viale Regina Elena 299, I-00161 Roma, Italy. Tel.: +39-06-4990-2243/2347; fax: +39-06-4938-7075.
E-mail address: garibaldi@iss.infn.it (F. Garibaldi).

0168-9002/$ - see front matter © 2004 Elsevier B.V. All rights reserved.
doi:10.1016/j.nima.2004.03.072

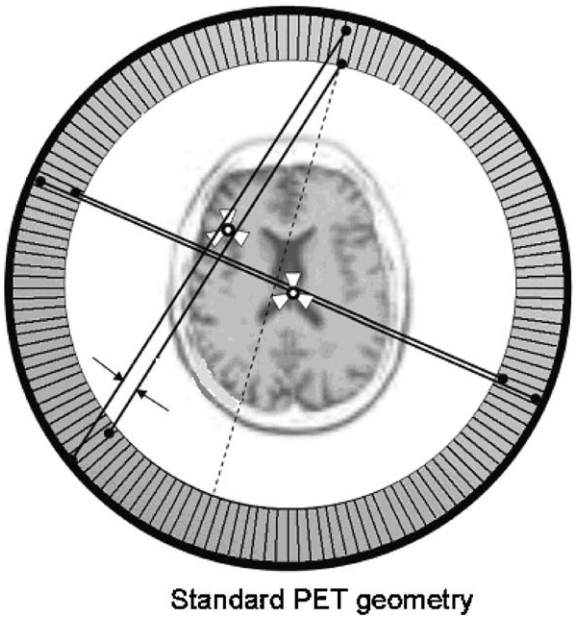

Fig. 1. Schematic drawing of a PET device. The parallax error, influencing emission points far from the ring centre, is schematically shown.

Nowadays there is a great effort to make PET devices with increased sensitivity and improved spatial resolution. This is dictated from the needs of imaging single organs (brain, breast, prostate, etc.) and small animals. In this case, the technique shows its actual limitations. Two main physical factors limit the PET spatial resolution: the positron range and the annihilation photons' non-collinearity. Moreover, there is another limiting factor owing to the penetration of the 511 keV photons into the crystals (Fig. 1). A photon impinging on the entrance face of a detector with an oblique angle with respect to its axis can be detected not in that detector, but in an adjacent one. This effect causes the parallax error, which increases with the distance of the positron emission point from the centre of the tomography ring [3]. This error can be significantly reduced or eliminated if the interaction point of the photon along the detector, i.e. the depth of interaction (DOI), can be measured.

Up to now, different approaches have been attempted to solve the DOI problem [1], such as the phoswich approach [4–6] (two different time decay constant scintillators piled up in radial direction), implemented in "the high-resolution research tomography" (HRRT) [4], or the detector stack approach, consisting in several layers of 2D photon detectors stacked in a 3D device. A third approach is based on the detection of the light reaching the two opposite bases of a scintillator. Many combinations of photodetectors have been used, including PIN photodiodes, APDs or PSPMTs [1]. Nevertheless, each of these photodetectors has intrinsic limitations (pixel size, number of pixels, surface coverage, energy resolution, gain uniformity), which compromise the final PET performance.

Our proposed PET scanner design employs the DOI approach, associated to the use of hybrid photon detector (HPD) photodetectors to solve the cited photodetector limitations.

2. PET hybrid photon detector concept

The proposed 3D axial PET scanner[1] (see Fig. 2), consists of axially oriented arrays (see Fig. 3) of long (100 mm) scintillator crystals of small cross-section ($3.2 \times 3.2\,mm^2$) with gaps of 0.8 mm between crystals. Each matrix (13 rows, 16 columns of scintillators) is read out on both sides by an HPD [5,6]. The size and segmentation of the silicon sensor of the HPD match exactly with the crystal matrix. This highly segmented geometry provides an accurate and uniform spatial resolution in the transaxial ($x-y$) plane, completely independent of the radial detector thickness. The transaxial segmentation allows tracking multiple interactions of annihilation photons in the scintillator matrix, which allows one to reconstruct a fraction of events which underwent Compton scattering in the detector. The axial coordinate (z) is derived with good precision from the ratio of the light intensities detected by the two HPDs at the ends of each scintillator matrix. This leads to a full 3D image reconstruction without any parallax effect, irrespective of the position of the annihilation point, which results in an enhanced PET

[1] Patent applied by CERN under publication number PCT/EP 02/07967.

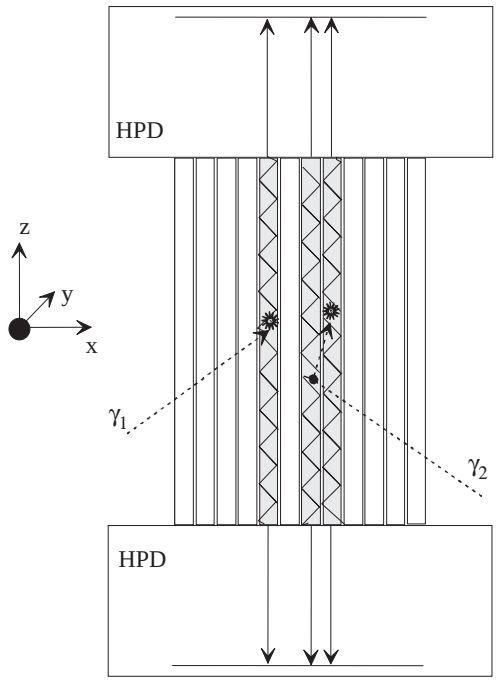

Fig. 2. Schematic view of a 3D axial PET camera module based on a scintillator matrix read out by two HPDs.

spatial resolution, uniform over the whole detection volume and improves the sensitivity owing to the Compton enhancement.

3. Choice of the scintillator

The x, y coordinate resolution depends only on the crystal segmentation and not on its constituent materials. The z resolution is instead linked to the choice of the scintillator and to its properties, in particular to its light yield and light absorption length. Properties like photofraction, decay time, market availability, machinability, price, etc. play of course also an important role when choosing a scintillator. In this first project phase, YAP:Ce has been chosen for the module tested in this work for its low cost, even if, compared to other scintillators, YAP has a low Z, a high absorption length, and a low photofraction. LSO:Ce and $LABr_3$:Ce scintillators would have been better candidates and will be studied later. All performance estimates and results in this paper refer to the use of YAP scintillators.

4. Hybrid photon detector

The HPDs designed for the PET prototype camera have a circular thin (1.8 mm) entrance window made of sapphire. They are equipped with semi-transparent bialkali photocathodes, which exhibit a quantum efficiency of about 25% at the wavelength of maximum emission of 370 nm. The electron optics of the HPD is such that a 1:1 image of the photon pattern on the photocathode is transferred to the silicon sensor ("proximity focusing"). The silicon sensor is segmented into 216 individual diodes of dimension $4 \times 4\,mm^2$ matching the pattern of the crystal matrix. The HPD is operated at a moderate potential difference between the photocathode and the silicon sensor of about 12 kV. Photoelectrons of 12 keV produce on average in the silicon sensor about 3000 electron–hole pairs with a spatial spread of 0.3 mm. The integrated self-triggering electronics, the VLSI chip VATA-GP, produced in 0.6 μm CMOS technology, is mounted on the ceramic carrier, which supports also the silicon sensor. Each of the 128 channels of this chip has a charge integrating preamplifier, a shaper, a tunable shaping time, and a readout register. A parallel fast shaper circuit ($\tau_s = 150$ ns) produces a trigger signal for the readout logic. The chip features also a sparse readout option, which allows achieving event rates of the order of several MHz. The single photoelectron efficiency of the HPD electronics is expected to be 93% .

5. PET performance estimates

Calculations and simulations using GEANT4 and EGS4 codes have been performed in order to characterize the performance of the system [8]. The number N_{rec} of photoelectrons in an HPD is determined by the number of produced scintillation photons N_{ph} at the z scintillation point in the crystal (length L) and the crystal attenuation length Λ': $N_{rec} = N_{ph}[(\exp(-z/\Lambda') + \exp(L -$

Fig. 3. A PET scanner comprising 12 camera modules with a free inner diameter of 34 cm, suited for brain diagnostics. The shape of the HPDs has been optimized to increase the active area coverage.

z/Λ')]. The energy resolution is given by the quadratic sum of the scintillator, statistical, and noise contributions. R_{sci} is equal to 2.5%, R_{noise} is negligible, and $R_{\text{stat}} = [0.5/E(\text{MeV})]^{1/2}6.5\%$. R_{stat} is equal to 7.5% for photons of 511 keV, while it is 16% for photons of 100 keV (all values correspond to FWHM).

The $x-y$ spatial resolution is given by the thickness s of the crystals: $\sigma_x = \sigma_y = s/\sqrt{12}$ (RMS). The z resolution, as will be discussed in Section 8, is related to the light absorption length and the light yield of the crystal.

6. Compton enhanced reconstruction

The transaxial segmentation allows tracking multiple interactions of annihilation photons in the scintillator matrix, which provides the possibility to reconstruct a fraction of events which were Compton scattered in the detector. Monte-Carlo simulations show that part of the events undergoing Compton scattering before photoelectric absorption can be reconstructed if the photons are scattered at forward angles ($10^\circ < \theta < 60^\circ$). Photons scattered larger angles are "ambiguous" and cannot be reconstructed. In YAP the photofraction at $E_\gamma = 511$ keV is only 3.8%. The simulations performed with EGS4 and GEANT4 show that nearly 8.7% of photons undergo a double interaction. Nevertheless, 3.5% can be correctly reconstructed, thus enhancing the coincidence efficiency of a factor 2 [7]. In case of LSO crystals, the enhancement due to Compton reconstructed events is less than a factor of 2, but the photoelectric fraction is much higher than YAP, being nearly 30%.

7. First results from measurements of optical properties of YAP:Ce crystals

Two matrix modules are under construction. YAP crystals have been procured from Crytur

Ltd. (Turnov, Czech Republic). All crystals have dimensions $3.2 \times 3.2 \times 100\,\mathrm{mm}^3$ with a maximum deviation from the nominal values of 0.03 mm. The optical polishing of all the surfaces is better than 10 nm (RMS), and by visual inspection they look free from scratches and inclusions.

The transmittance of light through one sample (3.2 mm), as measured by means of a Perkin-Elmer Lambda 9 spectrophotometer, is constant around 380 nm where YAP crystals with 0.05–0.1% Ce (weight fraction) have the luminescence peak which is nearly 60 nm wide. Because of the high refractive index of YAP the transmittance measurements are dominated by the reflection loss at the crystal–air interface.

The light absorption length of a YAP crystal has been measured through the ratio of the light seen by two PMTs mounted on each base of one crystal irradiated by a ^{137}Cs (662 keV photons) radioactive source. The used PMTs have standard bialkali photocathodes. Their quantum efficiency matches well the emission wavelengths of the YAP. The crystal has not been wrapped, but the ensemble crystal-PMTs have been encapsulated in a light tight black cylindrical box with a diameter of nearly 5 cm. The timing of the signals from the PMTs is deduced through CFDs. Coincident right-left signals have their amplitudes (Q_R, Q_L) and timings digitalized (ADC, TDC) and recorded by a multi-parametric acquisition system. The measurements yield the effective (Λ') and not the bulk (Λ) attenuation length. These are linked by the factor K which takes into account that the light propagates through the crystal by total internal reflection from the side walls: $\Lambda' = \Lambda K$. The value of K, evaluated through Monte-Carlo calculations, is ~ 0.8. Due to the small section of the crystal, the spectrum of detected photons is dominated by the Compton spectrum (see the first and second panels of Fig. 4). The photons completely stopped by the crystal are hardly seen in the left or right PMT spectra. But their presence (4.0% of the total photons) is clearly visible in the sum spectrum. The energy resolution of the photopeak is $\sigma_E/E = 4.3\%$. This value has been obtained with the source placed in the centre of the crystal ($z = 5$ cm), and, as will be seen later, varies slowly when changing the source position. The effective attenuation length ($\Lambda' = K\Lambda$) can be deduced from the sum of right and left PMT signals $Q_R + Q_L = N_{ph}(\exp(-z/\Lambda') + \exp(L - z/\Lambda'))$ (see Fig. 5) for different positions of the radioactive source, and from the ratio of left to right signals $Q_R/Q_L = (\exp(L - 2z/\Lambda'))$. The ratio (see Fig. 6) can also be deduced for photoeffect events only or by selecting only events at the Compton edge. The three analyses lead to the consistent values $\Lambda' = 223 \pm 9$, 217 ± 6, and 206 ± 8 mm. From their average and from the estimation of K, a bulk attenuation length of $\Lambda = 279 \pm 6$ mm is deduced.

The z position uncertainty $\sigma_z = \Lambda'/2[(Q_R + Q_L)(Q_R Q_L)]^{1/2}$, varies slightly with z and deteriorates with increasing Λ'. On the contrary, the energy resolution (σ_E) improves with increasing Λ'. From the measured Λ', we derive $\sigma_z = 5$ mm, a value which is clearly not sufficient for a competitive PET scanner. The expected energy resolution is $\sigma_E/E = 2.8\%/\sqrt{E}$ (E in MeV).

While a long light absorption length is generally preferable for a scintillator, in our specific geometry a shorter absorption length, e.g.

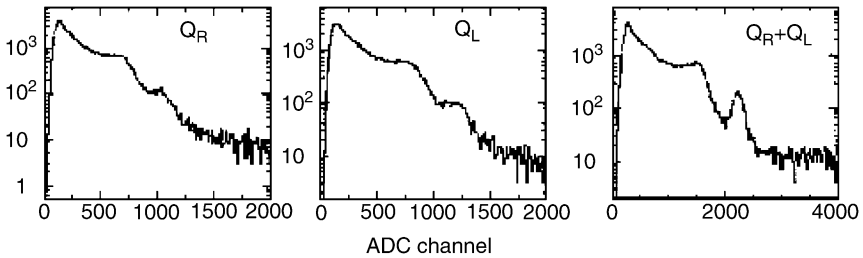

Fig. 4. Pulse height spectra of the right (Q_R) and left (Q_R) PMT as well as sum spectrum ($Q_R + Q_L$). The ^{137}Cs source was placed in the middle of the YAP crystal.

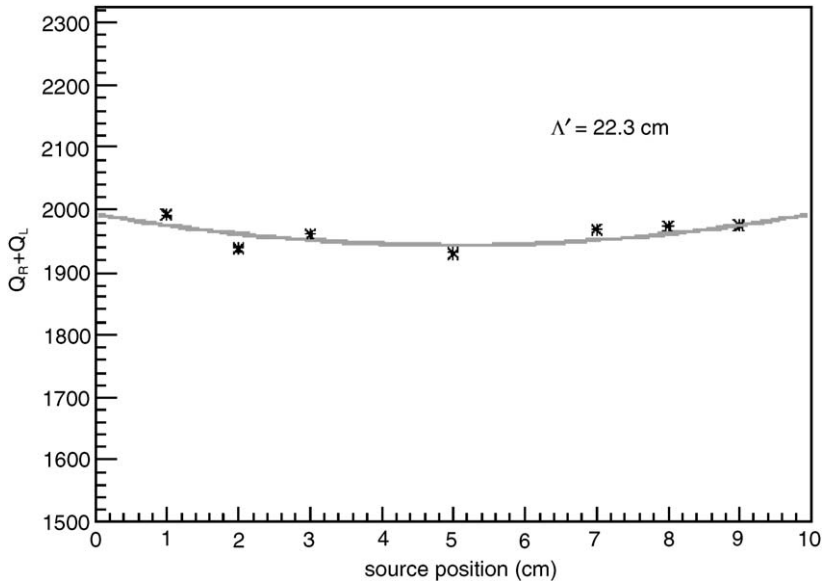

Fig. 5. Sum of left and right PMT signals ($Q_R + Q_L$) versus position of the ^{137}Cs source on the YAP crystal.

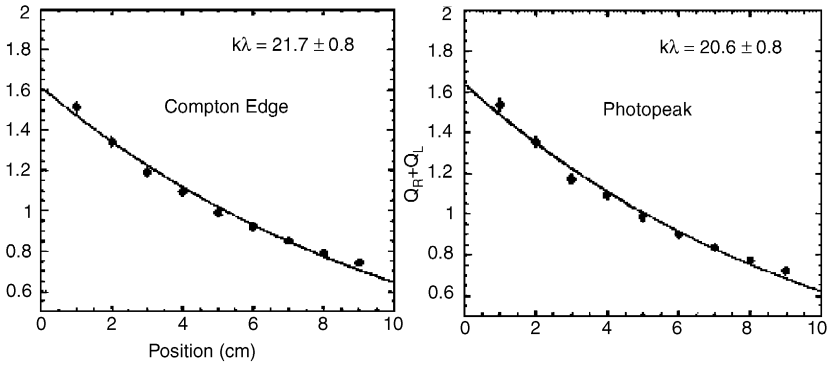

Fig. 6. Ratio Q_R/Q_L analysed for photons in the Compton edge region (left) and in the photopeak (right).

$\Lambda = 75$ mm, would significantly improve the position resolution ($\sigma_z = 2.8$ mm) and still lead a very good energy resolution $\sigma_E/E = 3.8\%/\sqrt{E}$. Three ways have been suggested to decrease the effective absorption length Λ': (1) change of the Ce concentration in the crystal (this actually reduces Λ itself, but requires to grow new crystals), (2) reduction of the surface reflectivity by chemically de-polishing, (3) coating the crystal lateral surfaces with a metal film in order to use the metallic reflectivity, instead of the total internal reflection.

Other measurements are under preparation for a first evaluation of the z coordinate precision in a crystal matrix. A prototype made by an array of YAP scintillators coupled with Hamamatsu R5900-M16 PSPMTs (the HPDs are not yet available) will be used. These PSPMTs have anode pixels with a size of $4 \times 4\,\text{mm}^2$, which match the dimensions of the crystal matrix. A pulsed light source will be used for the calibration of the single photoelectron pulse height.

8. Conclusions

A novel concept PET detector module has been proposed, which provides full 3D gamma reconstruction with high resolution over the total detector volume, free of parallax errors. The concept will first be proved with YAP:Ce crystals, then with other scintillators (e.g. LSO, LuAP, $LaBr_3$) better matching the PET needs. A possible application, currently under study, is a high-resolution brain PET with an axial field of view of 10–15 cm. Other applications, like PE mammography (PEM) and combination with other modalities or techniques, are also under investigation. Two prototypes of YAP scintillator arrays that will be used for the first PET prototype have been assembled and the characterization of their optical properties has started.

References

[1] W.W. Moses, Nucl. Instr. and Meth. A 471 (2001) 209.
[2] M.E. Phelps, J. Nucl. Med. 41 (2000) 661.
[3] M.E. Phelps, S.R. Cherry, Clin. Pos. Imag. 1 (1998) 31.
[4] K. Wienhard, M. Schmand, M.E. Casey, et al., IEEE Trans. Nucl. Sci. 49 (2002) 104.
[5] S. Surti, J.S. Karp, L.-E. Adam, et al., 2001. Performance measurements for the GSO-based brain PET camera (G-PET), in: Proceedings of the IEEE Nuclear Science Symposium and Medical Imaging Conference, San Diego, CA, October 4–10, pp. 1109–1114.
[6] M. Watanabe, K. Shimizu, T. Omura, et al., IEEE Trans. Nucl. Sci. 49 (2002) 634.
[7] A. Braem, et al., Novel design of high resolution parallax-free Compton enhanced PET scanner dedicated to brain research, in: Proceedings of the First International Meeting on Applied Physics, Badajoz, Spain, October 2003.
[8] A. Braem, E. Chesi, P. Hammarstedt, et al., Nucl. Instr. and Meth. A 497 (2003) 202.